Article

Cell

Cell-to-Cell Variation in p53 Dynamics Leads to Fractional Killing

Graphical Abstract

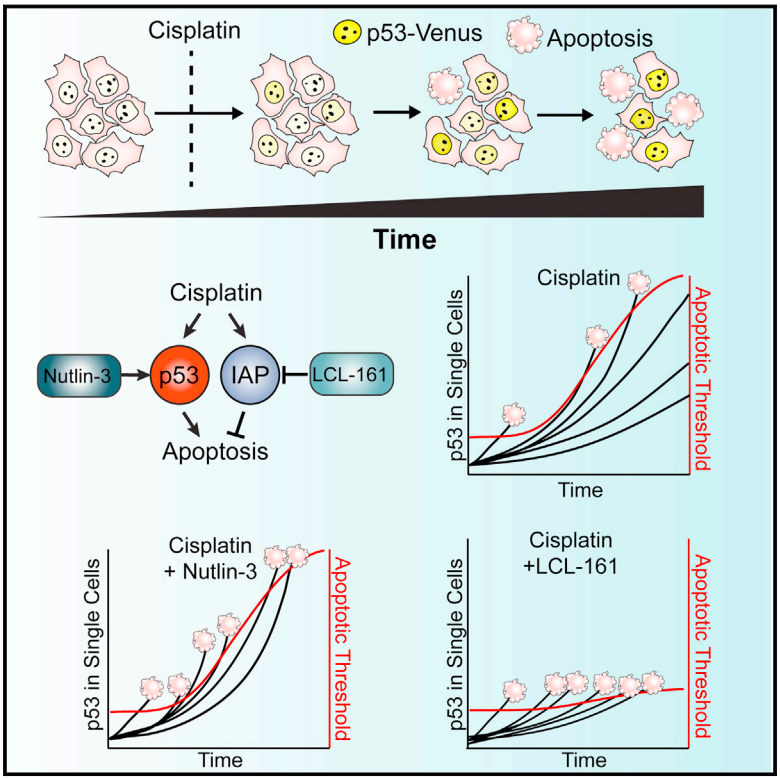

Highlights

- In response to a drug, single cells show different fates and rates of p53 induction
- The p53 threshold required to enact apoptosis rises with time
- Drug efficacy is enhanced by accelerating the rate of p53 induction
- Inhibition of anti-apoptotic proteins reduces the increase in threshold over time

Authors

Andrew L. Paek, Julia C. Liu, Alexander Loewer, William C. Forrester, Galit Lahav

Correspondence

galit@hms.harvard.edu

In Brief

Upregulation of p53 in response to chemotherapy leads to apoptosis in some cells while other cells survive. Cells with rapid induction of p53 enact apoptosis while cells with slow yet high levels of p53 survive due to the upregulation of IAP proteins. Cell death can be enhanced by either increasing the rate of p53 accumulation or flattening the p53 apoptotic threshold.

Paek et al., 2016, Cell *165*, 1–12
April 21, 2016
http://dx.doi.org/10.1016/j.cell.2016.03.025

CellPress

Please cite this article in press as: Paek et al., Cell-to-Cell Variation in p53 Dynamics Leads to Fractional Killing, Cell (2016), http://dx.doi.org/10.1016/j.cell.2016.03.025

Cell

Cell-to-Cell Variation in p53 Dynamics Leads to Fractional Killing

Andrew L. Paek,[1] Julia C. Liu,[1] Alexander Loewer,[1,3] William C. Forrester,[2] and Galit Lahav[1,*]
[1]Department of Systems Biology, Harvard Medical School, Boston, MA 02115, USA
[2]Developmental and Molecular Pathways, Novartis Institutes for Biomedical Research, Cambridge, MA 02139, USA
[3]Present address: Department of Biology, Technical University Darmstadt, 64287 Darmstadt, Germany
*Correspondence: galit@hms.harvard.edu
http://dx.doi.org/10.1016/j.cell.2016.03.025

SUMMARY

Many chemotherapeutic drugs kill only a fraction of cancer cells, limiting their efficacy. We used live-cell imaging to investigate the role of p53 dynamics in fractional killing of colon cancer cells in response to chemotherapy. We found that both surviving and dying cells reach similar levels of p53, indicating that cell death is not determined by a fixed p53 threshold. Instead, a cell's probability of death depends on the time and levels of p53. Cells must reach a threshold level of p53 to execute apoptosis, and this threshold increases with time. The increase in p53 apoptotic threshold is due to drug-dependent induction of anti-apoptotic genes, predominantly in the inhibitors of apoptosis (IAP) family. Our study underlines the importance of measuring the dynamics of key players in response to chemotherapy to determine mechanisms of resistance and optimize the timing of combination therapy.

INTRODUCTION

Chemotherapy resistance remains a major obstacle to effective cancer treatment. Considerable effort has been put forward to understand mechanisms of resistance in order to disrupt them and improve patient outcomes. In many cases, resistance has been linked to specific mutations in a subset of tumor cells, allowing them to survive chemotherapy treatment (Holohan et al., 2013). Investigations into isogenic populations of tumor cells reveal that resistance also emerges through non-genetic mechanisms, often through stochastic fluctuations in key factors in response to the drug (Cohen et al., 2008; Kreso et al., 2013; Roesch et al., 2010; Roux et al., 2015; Sharma et al., 2010; Spencer et al., 2009). Resistance can last days in some cases (Flusberg et al., 2013) and weeks in others (Sharma et al., 2010).

For many cancer types, the p53 transcription factor is a key player in the cellular response to DNA damage induced by chemotherapy (Figure 1A) (Vazquez et al., 2008). DNA-damaging agents disrupt the interaction between p53 and its transcriptional target and negative regulator Mdm2, leading to stabilization of p53 (Haupt et al., 1997). Increased abundance of p53 triggers the transcription of multiple genes in various downstream programs, including apoptosis and cell-cycle arrest (Riley et al., 2008). Previous studies have suggested a threshold mechanism where the choice between alternative programs depends upon p53 protein levels (Chen et al., 1996; Kracikova et al., 2013). In these models, low levels of p53 trigger cell-cycle arrest and high levels of p53 lead to apoptosis. In addition, p53's affinity for different target genes was shown to depend on the presence of specific transcriptional co-factors or post-translational modifications (Das et al., 2007; Samuels-Lev et al., 2001; Tang et al., 2006, 2008). More recently, we have shown that the dynamics of p53 play a role in the specificity of the response with pulsed p53 favoring DNA repair and cell-cycle arrest genes and sustained p53 triggering activation of senescence and apoptotic genes (Batchelor et al., 2011; Purvis et al., 2012). The variation in p53 dynamics between individual cells and the potential effect of such variation on the heterogeneous response to chemotherapy has not been explored.

Here, we studied the role of p53 dynamics in the fractional killing response to chemotherapy drugs with a focus on cisplatin. Cisplatin is a widely used chemotherapeutic drug that forms both inter and intra-strand DNA crosslinks as well as protein-DNA crosslinks that are highly toxic to rapidly dividing cancer cells (Kelland, 2007). Human colon cancer cells treated with intermediate doses of cisplatin show a heterogeneous response; a fraction of cells die while others enact cell-cycle arrest (Figure 1B) (Berndtsson et al., 2007). By quantifying p53 levels in single cells treated with cisplatin, we found a strong link between apoptosis and the dynamics of p53. Specifically, apoptotic cells accumulated p53 earlier and faster than surviving cells. Our analysis revealed that cells must reach a critical threshold level of p53 in order to enact apoptosis and this threshold increases with time following drug treatment.

We further showed that the increase in the apoptotic threshold over time is not due to diminished p53 activity but instead is linked to the upregulation of genes in the inhibitors of apoptosis (IAP) family. LCL-161, a small molecule that inhibits IAP proteins and is currently under clinical trials, significantly abolished the increase in the p53 apoptotic threshold with time. Increased IAP expression inhibits two separate apoptotic pathways that are differentiated by their dependence on caspase-8/Rip1. Our work points to p53 dynamics as a critical node underlying resistance to cisplatin and highlights the importance of studying individual cell behaviors for designing efficient drug combinations.

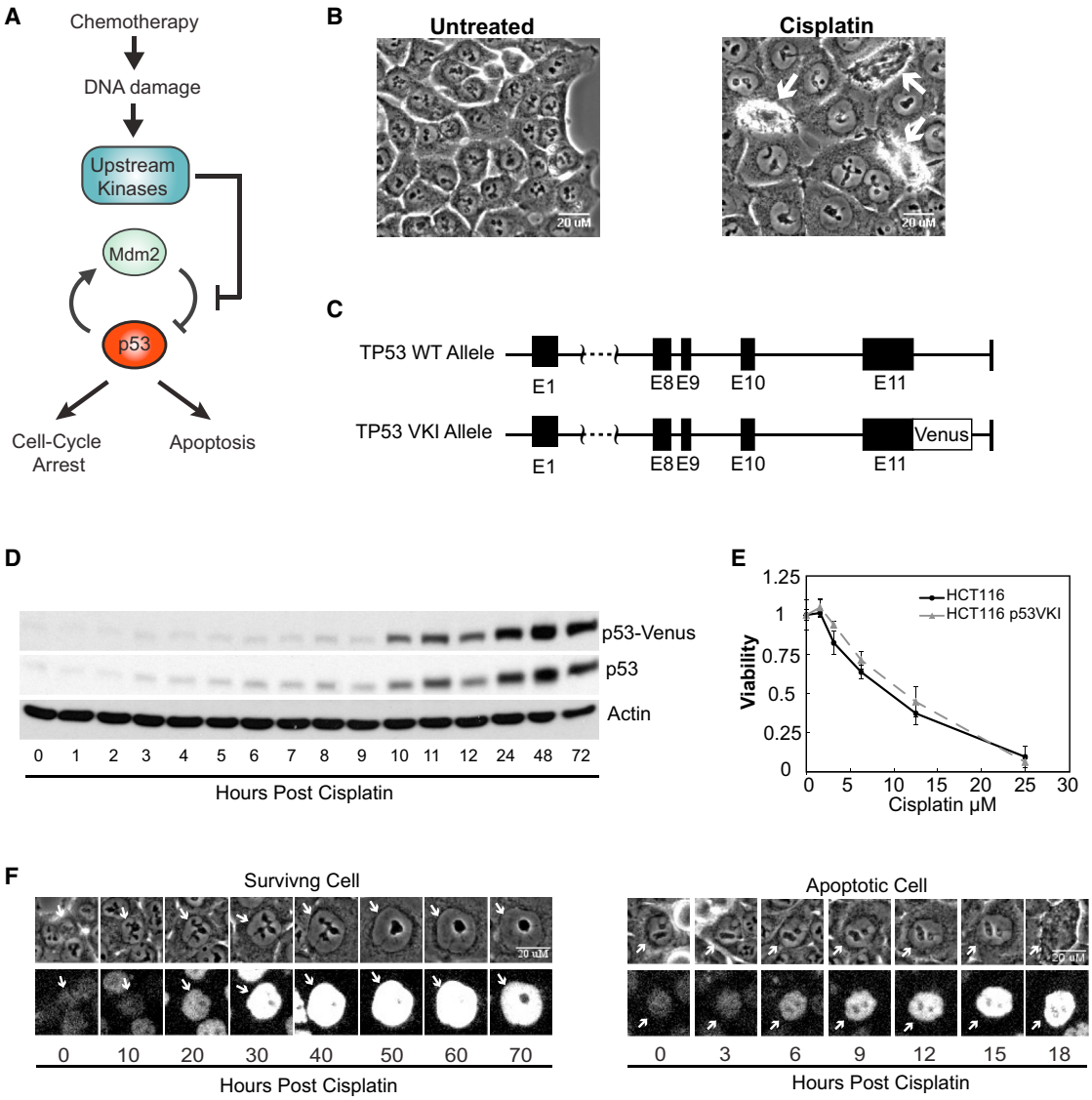

Figure 1. A System to Track p53 Levels in Single Cells

(A) Network diagram of the p53 response to chemotherapy treatment. p53 promotes the transcription of Mdm2, which binds p53 and tags it for degradation. DNA damage activates kinases that disrupt the interaction between p53 and Mdm2, leading to stabilization and accumulation of p53. Stabilized p53 promotes cell-cycle arrest and apoptosis.

(B) Images of unperturbed HCT116 cells (left panel) and in response to cisplatin (right panel). Cisplatin induces apoptosis in a fraction of cells (white arrows).

(C) Diagram of *TP53* alleles in the HCT116 p53-VKI cell line.

(D) Western blot of p53-Venus and untagged p53 levels in response to 12.5μM cisplatin. Actin was used as a loading control.

(E) Survival curve of HCT116 cells and p53-VKI cells 72 hr after cisplatin treatment, measured by Cell Titer-Glo. Error bars represent the SD of four replicates.

(F) p53 dynamics and cell fate were measured by live-cell microscopy. Apoptotic cells were identified visually, in the bright-field channel (right panel, hour 18) and p53 levels were quantitated from the fluorescence channel. Images were captured every 30 min for 72 hr.

See also Figure S1.

RESULTS

A System to Quantify p53 Dynamics and Cell Fate in Single Cells

We developed a system to measure p53 dynamics and cell fate in single human colon cancer cells (HCT116) following cisplatin treatment. Cisplatin was previously shown to induce p53-dependent apoptosis in HCT116 cells (Berndtsson et al., 2007; Zhu et al., 2013). We created an isogenic HCT116 p53 Venus knock-in cell line (p53-VKI), in which one allele of *TP53* is tagged with a Venus fluorescent protein at the C terminus of exon 11 (Figure 1C). The other allele of *TP53* is wild-type and unaltered. We verified that p53-Venus levels mimicked induction of endogenous p53, indicating that the Venus tag does not alter the

Please cite this article in press as: Paek et al., Cell-to-Cell Variation in p53 Dynamics Leads to Fractional Killing, Cell (2016), http://dx.doi.org/10.1016/j.cell.2016.03.025

regulation of p53 dynamics in response to cisplatin (Figure 1D). In addition, survival curves revealed that parental HCT116 and p53-VKI cells show a similar dose-dependent decrease in viability in response to cisplatin (Figures 1E and S1A) indicating that Venus-tagged p53 does not alter p53 activity in response to cisplatin.

We treated HCT116 p53-VKI cells with cisplatin and measured nuclear p53-Venus levels and cellular outcomes (apoptosis or survival) in single cells (Figure 1F). Cells were tracked for 72 hr as apoptotic events had largely ceased by this time (Figures S1A and S1B). Cells that did not die enacted cell-cycle arrest (Figures 1F, S1E, and S1F). We observed induction of p53 in both apoptotic and surviving cells, yet there was substantial heterogeneity in the levels, rate, and timing of p53 induction between cells (Figures 1F and S1C).

Rapid Accumulation of p53 Is Associated with Cell Death

To determine what features of p53 dynamics are associated with apoptosis, we extracted multiple parameters from the p53 trajectory of each cell and compared these parameters between apoptotic and surviving cells (Figure 2A). We initially focused on 12.5 μM cisplatin as this provided equal population sizes of apoptotic and surviving cells in our experimental system (Figure S1D). We found that maximum p53 levels did not differ between apoptotic and surviving cells (Figure 2B), suggesting that cell death is not simply determined by a fixed p53 threshold. Time-integrated p53 was also not associated with cell death (Figure 2C). In fact, surviving cells showed higher integrated levels of p53 than apoptotic cells. This is likely because p53 traces of surviving cells last longer than traces of apoptotic cells (Figure S2A).

The rate of p53 accumulation was associated with cell death. Apoptotic cells showed a faster accumulation of p53 than surviving cells (Figure 2D) and a shorter time to reach half-maximal p53 levels (Figure 2E). This difference in rate was strongly reflected in the time it took for p53 to reach 2 SD above its basal levels (Figures 2A and 2F). By this measure, apoptotic cells accumulate p53 significantly earlier than cells that survived cisplatin treatment (Figure 2F). We refer to this metric as "p53 onset" and use it to describe the time of p53 induction throughout this paper.

In agreement with our previous work (Loewer et al., 2010), ~12% of cells show high basal levels of p53 before cisplatin treatment (Figure S2B). To test the role of these cells in contributing to the correlation between early p53 induction and cell death, we removed them from our dataset and re-analyzed the metrics in Figure 2A. This analysis revealed similar trends as the complete dataset (Figures S2C–S2G), suggesting that cells with high basal levels of p53 are not responsible for the differences between apoptotic and surviving cells.

To investigate the effect of cisplatin dose on p53 onset, we treated cells with half and double the IC_{50} concentration of cisplatin (Figures 2G–2I). Cells treated with a low concentration of cisplatin showed a later p53 onset and a decreased amount of cell death (Figures 2G and 2J), while a higher cisplatin concentration led to an earlier p53 onset and more cell death (Figures 2I and 2J). For all concentrations tested, apoptotic cells did not have higher maximum or integrated p53 levels, but did accumulate p53 earlier than surviving cells (Figures S2H–S2J). Similar trends were found in response to two other chemotherapy drugs, the topoisomerase I inhibitor camptothecin and the topoisomerase II inhibitor etoposide (Figure S3), suggesting that the correlation between early induction of p53 and cell death is not limited to cisplatin but rather general to other DNA damaging drugs.

To further explore the correlation between the timing of p53 accumulation and cell fate, we combined p53 traces from all three doses of cisplatin into a viability matrix that calculates the percentage of apoptotic cells given the time in which cells accumulated different levels of p53 (Figures 2K and 2L). To do this, we broke up each p53 trace into 5-hr time intervals. Within each time interval, we binned cells according to integrated p53 levels and determined what percentage of cells in each bin died in response to cisplatin. The resultant viability matrix shows the percentage of apoptotic cells given a specific range of p53 levels (y axis) and the time that cells reached that level (x axis). The matrix shows that within each time interval, cells with higher levels of p53 are more likely to die than cells with lower levels of p53 (Figure 2K). In addition, within each p53 level interval, cells that reached that level earlier had a higher probability of apoptosis. These data show that a cell's probability of death depends on both the timing and levels of p53 induction.

These results led us to propose that p53 must reach a critical threshold level in order to trigger apoptosis and that this threshold increases with time after cisplatin treatment. Therefore, cells that accumulate p53 slower must reach higher levels of p53 in order to induce apoptosis. Consistent with this, we found a positive correlation between the time of death and the integrated p53 levels of apoptotic cells (Pearson's R = 0.54; Figure S2K). In order to visualize how the p53 apoptotic threshold changes over time, we sought to plot a threshold that most accurately separates the apoptotic and surviving cells. To do this, we performed a logistic regression analysis on each time window of the viability matrix in Figure 2K. We then used this data to assess the level of p53 required in each time window for at least 75% of cells to die (Figure 2L). This analysis produced a threshold that increases with time and has an accuracy of 70% (Figure 2L). Fixed threshold models performed poorly in comparison to an increasing threshold (Figure S3M). Although some reached accuracies of ~54%, they used an arbitrarily low threshold that maximizes true positives at the expense of true negatives. Linear thresholds that maximized both true positives and true negatives were only ~40% accurate (Figure S3N). Note that while an increasing threshold more accurately predicts cell death than a fixed threshold, there is still an overlap in p53 dynamics in surviving and apoptotic cells (Figures 2K and 2L). This is likely due to fluctuations in other cellular factors that control apoptosis in response to DNA damage (e.g., Cohen et al., 2008).

Accelerating p53 Accumulation Early after Cisplatin Treatment Increases Cell Death

We experimentally tested the increasing threshold model by accelerating the rate of p53 accumulation at different times post cisplatin treatment and measuring the effect on cell fate (Figure S4). Acceleration of p53 was achieved using Nutlin-3, a small molecule that stabilizes p53 without further inducing DNA damage (Vassilev et al., 2004). Addition of Nutlin-3 to cells early in the response (5 hr after cisplatin treatment) led to an earlier p53

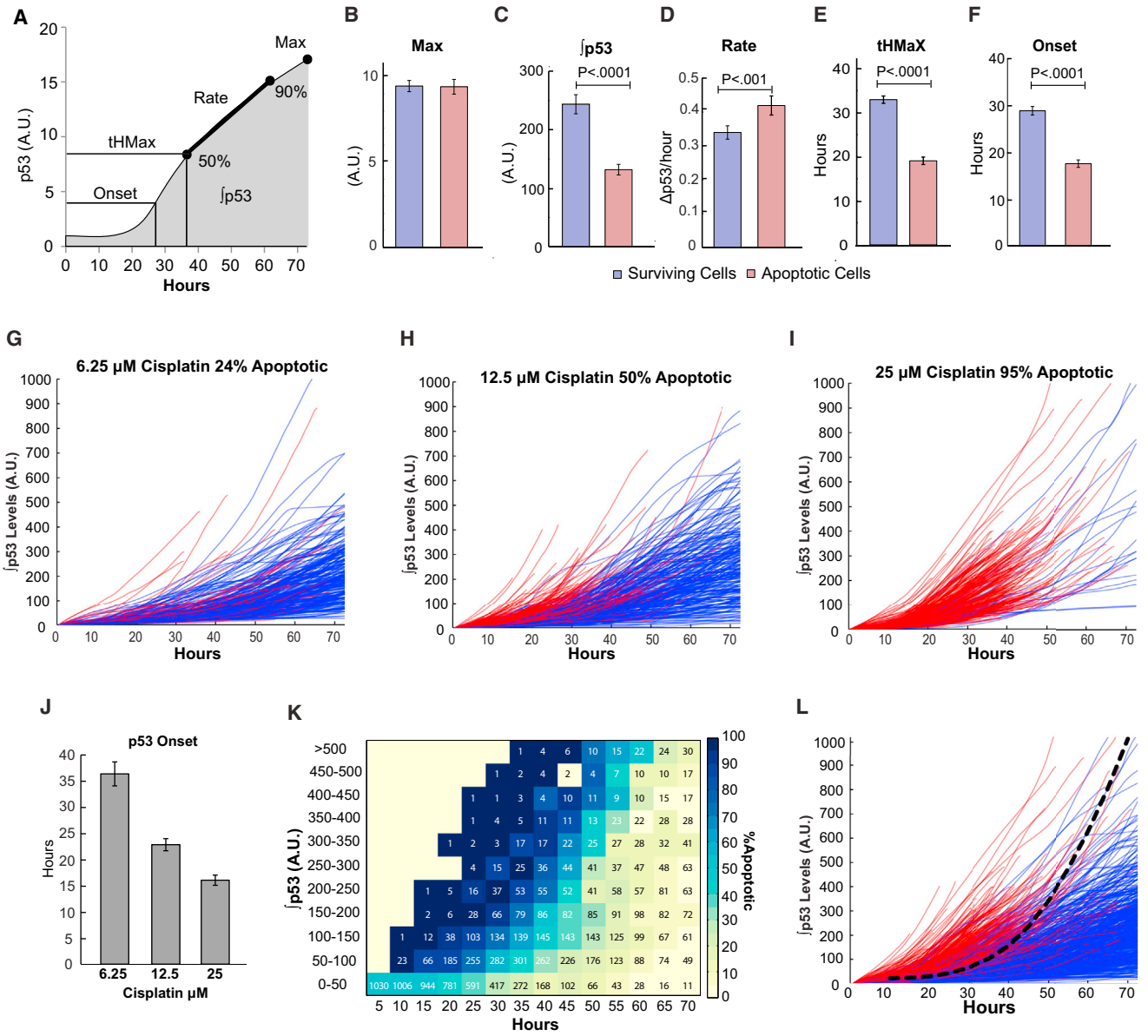

Figure 2. Cell Fate Depends on the Time and Level of p53 Induction

(A) Metrics used to distinguish p53 dynamics of apoptotic and surviving cells.

(B–F) Averages of each metric for surviving cells (blue) and apoptotic cells (red). Error bars represent the SEM. (B) Maximum p53 levels reached. (C) Total integrated p53 levels. (D) The rate of p53 accumulation, determined by linear regression on the points from 50% to 90% of the maximum and calculating the slope. (E) The time it took for each cell to reach half maximal levels of p53, and (F) the time p53 levels reached 2 SD above the mean at time 0, p53 onset.

(G–I) Single cell traces of integrated p53 levels in response to different concentrations of cisplatin. Apoptotic cells are in red, surviving cells in blue (G) 6.25 μM cisplatin (N = 297) (H) 12.5 μM cisplatin (N > 400), and (I) 25 μM cisplatin (N = 299).

(J) Average time of p53 onset for each cisplatin concentration.

(K) Viability matrix. Traces from all three cisplatin concentrations (N = 1,030) were binned in 5-hr time windows (x axis) and by integrated p53 levels (y axis). The color of each rectangle represents the percentage of apoptotic cells in each bin. Legend is on the right. The number in each rectangle is the number of cells in the bin.

(L) Single cell traces of integrated p53 levels from all three concentrations of cisplatin (N = 1,030). The dashed line represents the predicted apoptotic threshold and was calculated by performing logistic regression on each time window of the data from (K). Seventy-three percent of cells above the threshold were apoptotic (N = 534), and 34% of cells below the threshold were apoptotic (N = 496). p Values were calculated by a t test.

See also Figures S2 and S3.

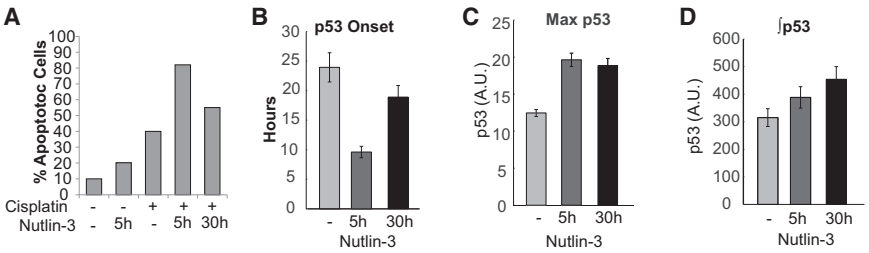

Figure 3. Early Accumulation of p53 Increases Cell Death

(A) Percentage of apoptotic cells for each treatment measured by time-lapse microscopy. N ≈ 100 cells per treatment.

(B–D) Average time of (B) p53 onset, (C) maximum p53 levels, and (D) integrated p53 levels for each treatment with and without 2 μM Nutlin-3. Values calculated as described in Figure 2. Error bars represent the SEM.

See also Figure S4.

onset and to a significant increase in the percentage of apoptotic cells (Figures 3A, 3B, and S4B). Interestingly, when cells were treated with Nutlin-3 late (30 hr after cisplatin treatment), p53 reached similar maximum levels and higher integrated levels than cells treated with Nutlin-3 early (Figures 3C, 3D, and S4C). However, late acceleration of p53 had only a modest effect on cell death (Figure 3A). These experiments support a model in which the potential for p53 to enact the apoptotic program decreases with time.

p53 Activates Apoptotic and Cell-Cycle Arrest Genes Regardless of the Time of Activation

What mechanistically moves the p53 threshold with time? We first asked whether p53 target genes in different programs respond differently to the time of p53 induction. Specifically, does rapidly-induced p53 favor the induction of apoptotic genes while slow accumulation of p53 favors cell-cycle arrest genes? To test the relationship between p53 dynamics and its target genes in different programs, we created a cell line expressing reporters for PUMA, a p53 target gene in the apoptosis pathway (Nakano and Vousden, 2001; Yu et al., 2001) and p21, a CDK inhibitor that causes cell-cycle arrest (Figure 4A) (el-Deiry et al., 1993). Both PUMA and p21 levels are increased by cisplatin treatment (Duale et al., 2007) and HCT116 PUMA$^{-/-}$ cells have reduced sensitivity to cisplatin (Jiang et al., 2006). We tracked PUMA and p21 induction in single cells after cisplatin treatment and quantified their dynamics together with p53 and cell fate (Figures 4B and 4C). We found that PUMA and p21 were induced in both apoptotic and surviving cells (Figures 4D and 4E). Moreover, we observed a positive correlation between integrated p53 levels and integrated PUMA and p21 levels (Figures 4F and 4G). This suggests that p53 accumulation simply translates into PUMA and p21 induction regardless of the time of p53 activation. Indeed, we found no correlation between the time of p53 onset and the level of PUMA or p21 expression (Figures 4H and 4I). These results show that the ability of p53 to transcribe apoptotic and cell-cycle arrest genes does not change over time, suggesting that other mechanisms are responsible for the increase in the p53 threshold required for apoptosis.

Cisplatin Upregulates Inhibitors of Apoptosis Proteins

Another possible mechanism for the increasing threshold is that cisplatin might upregulate anti-apoptotic proteins that antagonize p53-dependent apoptosis. In this scenario, slow accumulation of p53 allows time for apoptotic inhibitors to build up, compete with apoptotic genes, and prevent cell death. A buildup of apoptotic inhibitors increases the amount of p53 required to enact apoptosis. To identify putative anti-apoptotic genes that move the p53 threshold, we used a publicly available microarray dataset of HCT116 cells treated with cisplatin (Duale et al., 2007). We searched for genes that were significantly upregulated after cisplatin treatment ($p < 0.05$) and associated with negatively regulating apoptosis (GO: 0043066). This analysis revealed three genes from the inhibitors of apoptosis proteins (IAPs) family (cIAP1, cIAP2, and ML-IAP/LIVIN). Overexpression of IAP proteins was previously shown to decrease apoptosis in response to different DNA-damaging agents (Liston et al., 1996; Vucic et al., 2000). In addition, IAP proteins are frequently overexpressed in tumors and associated with poor patient survival and resistance to chemotherapy (Lopes et al., 2007; Nakagawa et al., 2006).

We measured the fold change in gene expression for the three IAP genes identified by the search, as well as XIAP, an additional member in the IAP family. Cisplatin led to an increase in the expression of all four IAP genes tested, with cIAP2 and ML-IAP showing the strongest induction (Figure 5A). Western blots confirmed an increase in all four IAP proteins in response to cisplatin (Figures 5B and 5C). Etoposide, camptothecin, and doxorubicin also caused a similar increase in IAP gene expression (Figure S5A). In addition, analysis of other microarray datasets (Altena et al., 2015; Hussner et al., 2012) revealed that induction of IAP genes after doxorubicin or cisplatin treatment occurs in other cancerous (HeLa; Figure S5B) and primary (HMEC-1; Figure S5C) cell lines. Together, these results suggest that induction of IAP proteins by DNA damaging agents is not limited to cisplatin or HCT116 cells (Figures S5A–S5C).

To further test the potential role of IAP proteins in preventing apoptosis following DNA damage, we expressed each of the four induced IAP genes from a constitutive CMV promoter (Figures S5D–S5G). Overexpression of each gene increased the viability of HCT116 cells following cisplatin treatment (Figure 5D). Consistent with these findings, CRISPR/Cas9 knockouts of cIAP1 and cIAP2 sensitized cells to cisplatin treatment (Figures 5E and S5H). Several attempts to knockout XIAP and ML-IAP were unsuccessful. We therefore used LCL-161, a small molecule that inhibits proteins in the IAP family by binding to a common BIR domain (Fulda and Vucic, 2012). LCL-161 alone had no effect on the viability of HCT116 cells, but a combination treatment of LCL-161 with cisplatin led to a significant decrease in viability (Figure 5F). Similar interactions were observed between LCL-161 and other DNA-damaging agents that induce the expression of IAP proteins (Figures S5A and S5I). Importantly,

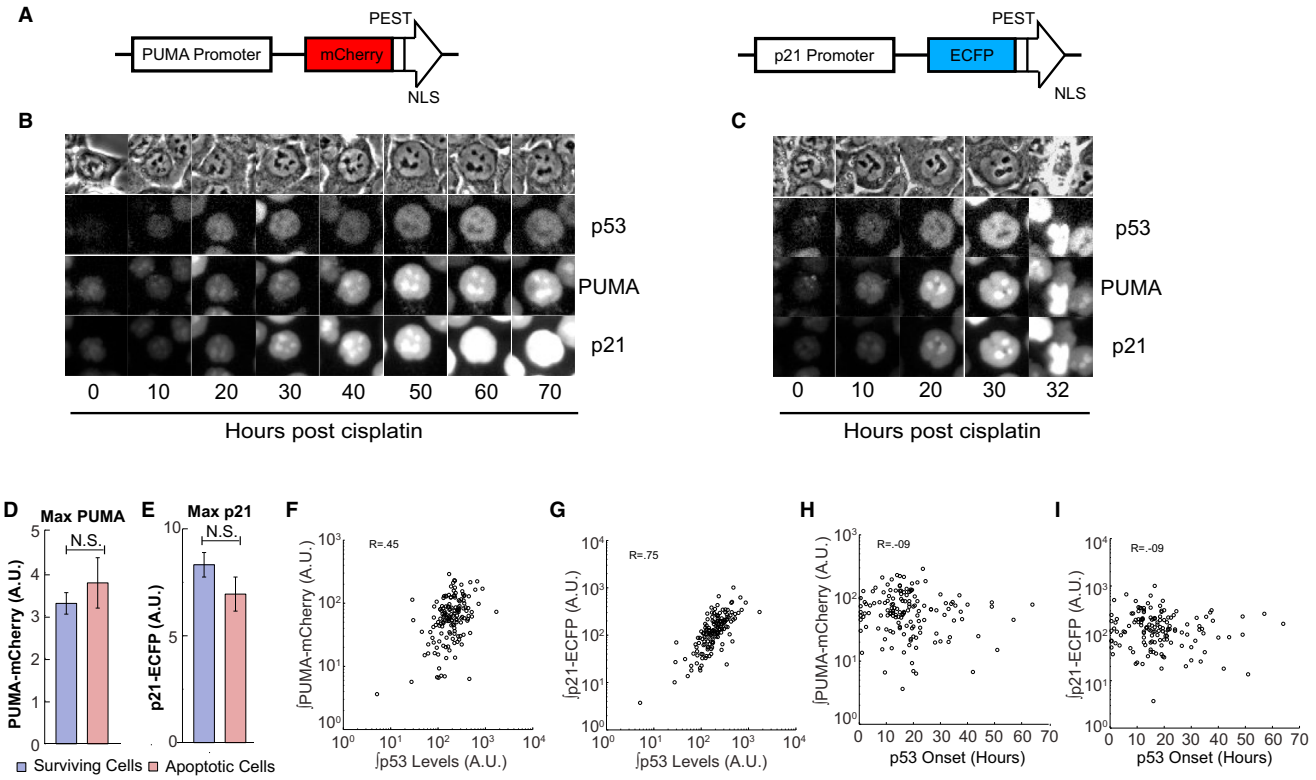

Figure 4. Induction of PUMA and p21 Are Not Correlated with the Time of p53 Induction

(A) Diagram of the reporters created to measure PUMA and p21 induction. NLS, nuclear localization signal.

(B and C) Sample images of (B) a surviving cell and (C) an apoptotic cell. Cells treated with 12.5 μM Cisplatin.

(D and E) Maximum PUMA-mCherry and p21-ECFP levels in surviving (blue) and apoptotic (red) cells. Error bars represent the SEM. N.S., not significant; p = 0.40 and 0.22, respectively.

(F and G) Integrated p53 levels versus integrated PUMA-mCherry (F) and p21-ECFP levels (G).

(H and I) The time of p53 onset versus (H) integrated PUMA-mCherry levels and (I) p21-ECFP levels in cisplatin-treated cells. R is the correlation coefficient.

the effect of LCL-161 on cisplatin-treated cells was p53-dependent (Figure 5F), supporting the hypothesis that upregulation of IAP proteins inhibits p53-dependent apoptosis.

IAP Inhibitors Flatten the Increase in the Apoptotic Threshold of p53

If induction of IAP proteins competes with p53 over time, then inhibition of these proteins should increase the time-window in which cisplatin is effective by flattening the apoptotic threshold. We tested this hypothesis using the IAP inhibitor LCL-161. In addition to LCL-161, we also separately tested the effect of ABT-263, a Bcl-2 family inhibitor. ABT-263 is known to lower the p53 apoptotic threshold (Kracikova et al., 2013), but unlike LCL-161, the targets of ABT-263 (BCL2, BCL-XL) show little or no induction by cisplatin (Figure 5G), suggesting that they do not contribute to the increase in the p53 apoptotic threshold with time. Similar to LCL-161, ABT-263 alone had no effect on the viability of HCT116 cells, but a combination treatment with cisplatin and ABT-263 led to a significant decrease in viability (Figure 5H). Single cell traces revealed that neither ABT-263 nor LCL-161 affected the timing of p53 accumulation (Figure S6A) or the maximum levels of p53 (Figure S6B).

We next produced a viability matrix for each dataset and performed logistic regression to measure how ABT-263 and LCL-161 affect the p53 apoptotic threshold over time (Figures S6C and S6E). As described above, cisplatin-treated cells showed a steady increase in the apoptotic threshold (slope = 15.2; Figure 2L). This was reflected by a positive correlation between the time of death and the integrated p53 levels of apoptotic cells (R^2 = 0.29; Figure S2K). Treatment with a combination of cisplatin and LCL-161 lowered the apoptotic threshold and most importantly made the threshold less time-dependent (slope = 4.3; Figures 5I and S6C). Consistent with this, we found no correlation between the time of death and integrated p53 levels (R^2 = 0.06; Figure S6D). Cells treated with cisplatin and ABT-263 showed a lower apoptotic threshold that still increases with time (slope = 10.5) yet at a lower rate than cisplatin alone, but faster than cells treated with cisplatin and LCL-161 (Figures 5J and S6E). In addition, there was a positive correlation between the time of death and integrated p53 levels in cells treated with ABT-263 and cisplatin (R^2 = 0.37; Figure S6F). Taken together, our results suggest that induction of anti-apoptotic genes, predominantly genes in the IAP family, compete with p53 and therefore increases the amount of p53 required to execute apoptosis with time.

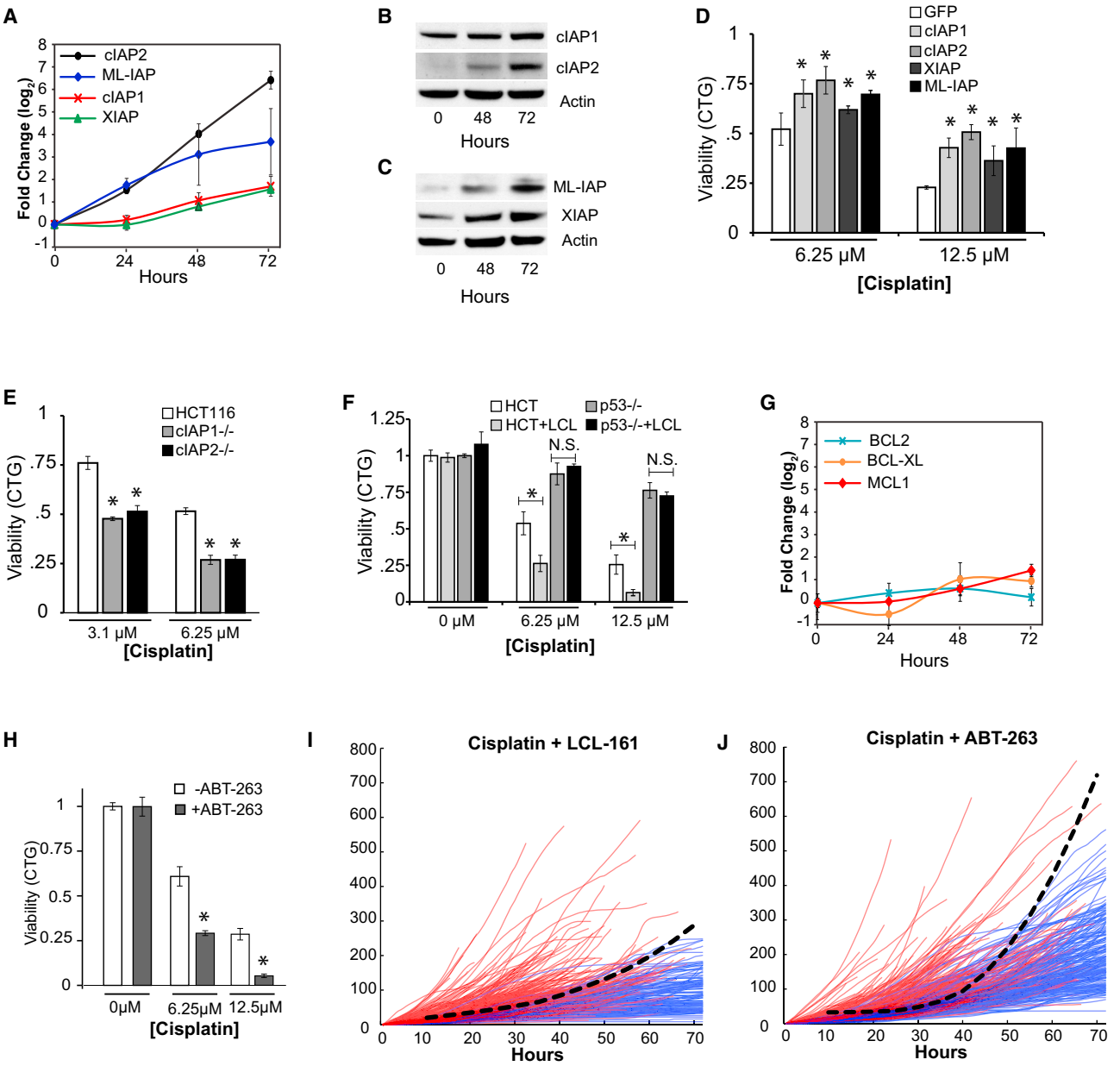

Figure 5. Cisplatin Upregulates Genes in the IAP Family that Compete with p53 and Limit the Time It Can Trigger Apoptosis

(A) Average $\log_2$ fold changes of IAP genes in response to 12.5 μM cisplatin measured by qPCR of three biological replicates.

(B and C) Western blot of cIAP1, cIAP2, ML-IAP, and XIAP after 12.5 μM cisplatin treatment. Actin was used as a loading control.

(D–H) CellTiter-Glo assays measured 72 hr after cisplatin treatment. (D) HCT116 cells were transfected with GFP, cIAP1, cIAP2, XIAP, or ML-IAP driven by a CMV promoter for 24 hr before cisplatin treatment. Data is normalized to untreated transfected cells. (E) HCT116, cIAP1$^{-/-}$ and cIAP2$^{-/-}$ cells treated with cisplatin. (F) HCT116 and HCT116 p53$^{-/-}$ cells treated with cisplatin and 1 μM LCL-161 (LCL). (G) Average $\log_2$ fold changes of Bcl2 family genes measured as in (A). (H) HCT116 cells treated with cisplatin and 200nM ABT-263.

(I and J) Single-cell traces of integrated p53 in response to (H) cisplatin + 1 μM LCL-161 and (I) cisplatin + 200 nM ABT-263. Apoptotic cells are red, surviving cells in blue. Dashed line represents the apoptotic threshold calculated by logistic regression on the viability matrix in S6C and S6E and assessing the p53 levels required for 75% of cells to die. The accuracy of the apoptotic threshold was 75% for cisplatin + LCL-161 and 68% for cisplatin + ABT-263. Error bars represent the SD. *Significant $p < 0.05$. N.S., not significant, calculated by a t test.

See also Figures S5 and S6.

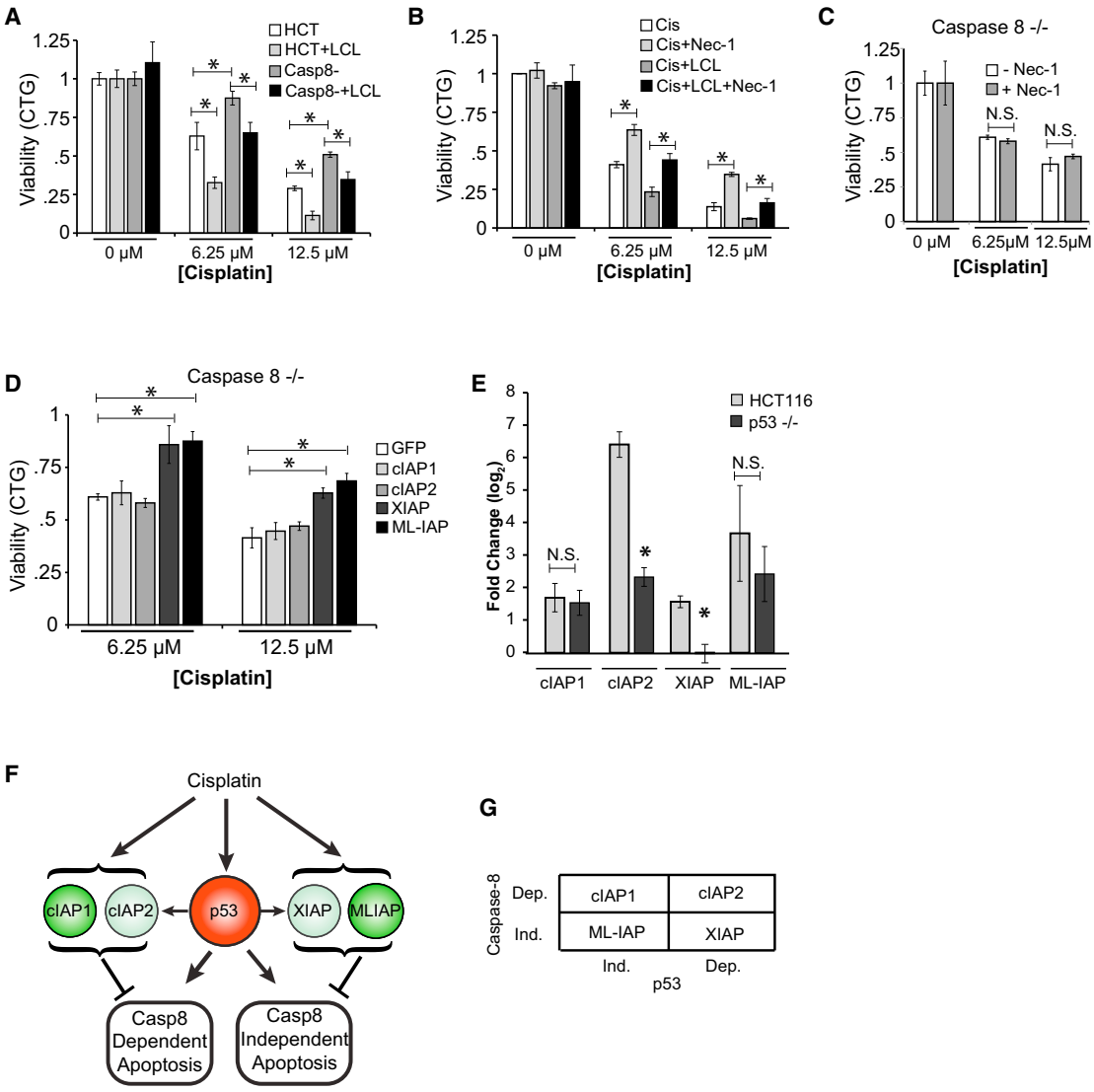

Figure 6. Cisplatin Induces Caspase-8-Dependent and -Independent Apoptotic Pathways

(A–D) CellTiter-Glo assays measured 72 hr after cisplatin treatment. (A) HCT116 (HCT) and HCT116 caspase $8^{-/-}$ (Casp8^{-}) cells treated with cisplatin and 1 μM LCL-161. (B) HCT116 cells treated with combinations of cisplatin, 1 μM LCL-161, and 30 μM necrostatin-1 (Nec-1). (C) Caspase $8^{-/-}$ treated with 30 μM necrostatin-1. (D) Caspase-$8^{-/-}$ cells transfected with CMV driven GFP, cIAP1, cIAP2, XIAP, or ML-IAP for 24 hr before cisplatin treatment. Data is normalized to untreated transfected cells.

(E) Average $\log_2$ fold changes of IAP genes in HCT116 and HCT116 $p53^{-/-}$ cells 72 hr after 12.5 μM cisplatin treatment.

(F) Cisplatin upregulates both pro and anti-apoptotic pathways that act on two different apoptotic pathways.

(G) Table showing the dependence of each IAP gene on p53 for transcription as well as whether the IAP gene inhibits caspase-8-dependent or -independent apoptosis. *Significant $p < 0.05$; N.S., not significant, as calculated by a t test.

IAP Proteins Suppress Separate Apoptotic Pathways, and Their Induction Is Partially Dependent on p53

Proteins in the IAP family are known to inhibit different apoptotic pathways. For example, cIAP1, cIAP2, and to some extent, XIAP, are known to inhibit an apoptotic pathway that involves caspase-8/RIP1/FADD (Tenev et al., 2011; Varfolomeev et al., 2007; Vince et al., 2007). In addition, both XIAP and ML-IAP are known to inhibit apoptosis either by direct binding and inhibition of caspases (XIAP) or by binding to Smac, a caspase activator (Fulda and Vucic, 2012). To test the relative contribution of each of these pathways to apoptosis after cisplatin, we first deleted caspase-8 using CRISPR/Cas9 (Figure S5J) and measured cell viability. We found that caspase-$8^{-/-}$ cells were less sensitive to cisplatin and to a combination of cisplatin with LCL-161 than wild-type cells (Figure 6A). Cells treated with the Rip1 kinase inhibitor Necrostatin-1 showed a similar pattern of cisplatin resistance (Figure 6B) that was caspase-8-dependent (Figure 6C). These results suggest that a fraction of cell death in response to cisplatin is caspase-8/Rip1-dependent.

In order to determine whether upregulation of IAP genes inhibits the caspase-8 independent pathway, we expressed each of the four induced IAP genes from a constitutive CMV promoter in caspase-8$^{-/-}$ cells. We found that both XIAP and ML-IAP overexpression significantly increased the viability of wild-type and caspase-8$^{-/-}$ cells (Figures 5D and 6D). In contrast, cIAP1 and cIAP2 overexpression protected wild-type cells, but had no effect on the viability of caspase8$^{-/-}$ cells after cisplatin treatment (Figures 5D and 6D). These data suggest that cisplatin induces cell death through two separate apoptotic pathways; one pathway is dependent on caspase-8/Rip1, while the other acts independent of caspase-8. Cisplatin also induces cIAP1/cIAP2 expression that prevents caspase-8-dependent apoptosis and ML-IAP/XIAP expression that inhibits caspase-8-independent apoptosis (Figure 6F).

Lastly, we asked whether p53 contributes to the anti-apoptotic arm in response to cisplatin and specifically to the induction of IAPs. Measuring the expression of IAP genes in wild-type and p53$^{-/-}$ lines following cisplatin treatment revealed that induction of two IAP genes (cIAP2 and XIAP) was reduced in a p53 null line, while induction of the other two IAP genes (cIAP1 and ML-IAP) was induced to similar levels (Figure 6E). Interestingly, the two p53-dependent genes include one gene that inhibits caspase-8-dependent apoptosis and one that inhibits caspase-8-independent apoptosis (Figures 6F and 6G). A similar pattern was found for the two p53-independent genes (Figure 6G). This analysis suggests a specific combination of regulation and function for each IAP gene induced by DNA damage (Figure 6G).

DISCUSSION

Chemotherapy is used to treat almost all types of cancer. Yet the response to chemotherapy is often incomplete, with a subset of cells surviving treatment (Almendro et al., 2013). The fraction of cells that die in response to chemotherapy increases with the dose, however, doses are limited by the toxic side effects to the patient. Consequently one potential way to improve patient outcomes is through increasing drug efficacy. An understanding of the source of heterogeneity within a tumor and how such heterogeneity contributes to resistance could lead to more effective treatment strategies. Here, we looked at the variation in the temporal behavior of p53 in single cells in response to cisplatin and other DNA damaging agents and asked how such variations are linked with cell-fate decisions. DNA damage activates p53, which in turn leads to the transcription of genes required for both cell-cycle arrest and apoptosis. Yet it is unclear why increased p53 levels lead to cell-cycle arrest in some cases and apoptosis in others (Carvajal and Manfredi, 2013) and why isogenic populations exhibit a mix of outcomes to the same stimulus.

We used live-cell imaging over multiple days to track p53 dynamics and cell fate in single colon cancer cells in response to chemotherapy treatment. This revealed that p53 must reach a critical threshold level in order to execute apoptosis, and this threshold increases over time. Consequently, cells that accumulate p53 slower must reach higher levels of p53 in order to enact apoptosis. We have also shown that enhancing the rate of p53 induction by Nutlin-3, a small molecule that inhibits Mdm2 and stabilizes p53, increases cell death (Figure 3). It is perhaps not surprising that stabilizing p53 leads to more cell death; however, we have also shown that the time at which Nutlin-3 is added after cisplatin is critical. Specifically, if Nutlin-3 is added too late then p53 levels are enhanced, yet this has a minimal impact on cell death (Figure 3). A recent study in triple-negative breast cancer cells revealed a similar dependence on timing when cells were treated with a combination of doxorubicin and erlotinib, an EGFR inhibitor (Lee et al., 2012). It is likely that other combination therapies can be optimized by altering the timing of drug additions. For p53 targeted therapy, many have suggested using Mdm2 inhibitors in combination with chemotherapy for treating tumors (Shangary and Wang, 2009; Vassilev, 2007). The results described in this study highlight the fundamental role that timing plays in such strategies.

Although time affected the p53 apoptotic threshold, it did not affect p53 transcriptional capability, as induction of p21 and PUMA were proportional to integrated p53 in single cells (Figure 4). Similar results were shown using population measurements after p53 induction with an inducible promoter (Kracikova et al., 2013). We have further shown that the increase in the apoptotic threshold over time was due to induction of genes in the IAP family by cisplatin and other DNA damaging agents (Figures 5 and S5). IAP proteins are commonly overexpressed in tumors and are associated with resistance to chemotherapy (Fulda and Vucic, 2012; Lopes et al., 2007) making them attractive candidates for targeted therapy. A number of different "Smac-mimetic" compounds have been developed to inhibit IAP proteins and sensitize cancer cells to chemotherapy (Fulda and Vucic, 2012). We showed here that one such compound, LCL-161, dramatically reduced the increase in the p53 apoptotic threshold (Figure 5). For this study, we focused on HCT116, a colon cancer cell line. Yet, it is likely that other cell lines also exhibit an increase in the p53 apoptotic threshold over time, as both HeLa cells and HMEC-1 cells induce genes in the IAP family after DNA damage (Figures S5B and S5C). An increase in the expression of IAP genes after DNA damage was also found in breast (Rashi-Elkeles et al., 2014) and thyroid (Tirrò et al., 2006) cancer lines. However, not all thyroid lines show increased induction of IAP genes, suggesting that the increase in the p53 apoptotic threshold with time might exist in some, but not all cell lines.

Our study raises the question of why both pro- and anti-apoptotic pathways are upregulated by the same stimulus. One possibility is that this allows cells to identify the magnitude of the damage and respond accordingly. DNA damaging agents do not lead to a fixed number of lesions in individual cells. Instead, cells vary in the number of lesions acquired (Liedert et al., 2006; Loewer et al., 2013). Cells that acquire a large number of lesions might reach high p53 levels rapidly and enact apoptosis before IAP proteins accumulate. Cells with few lesions will upregulate p53 slowly leading to cell-cycle arrest and slow accumulation of apoptotic proteins. This gives IAP proteins time to accumulate and prevent premature cell death. In support of this model, cells treated with low levels of cisplatin accumulate p53 slower than cells with high levels of cisplatin (Figures 2G–2J). Other factors likely contribute to differences in the rate of p53 accumulation, such as cell-cycle phase and the stochastic

fluctuation of proteins in the p53 network. Further studies are required to determine the contribution of potential factors to the heterogeneous rate of p53 induction in response to DNA damage.

Multiple pathways in a diverse set of organisms use dynamics to dictate distinct outcomes (Hao and O'Shea, 2011; Hoffmann et al., 2002; Kuchina et al., 2011; Lee et al., 2014; Purvis and Lahav, 2013; Toettcher et al., 2013; Young et al., 2013). In mammalian systems, proteins known to control outcomes through signaling dynamics are frequently associated with human disease. The ability to alter cell fate by modifying protein dynamics with combination therapies provides a novel therapeutic opportunity (Behar et al., 2013). A quantitative understanding of the dynamics of IAP proteins, how they vary between individual cells, and their relative rate in comparison to p53 induction rates, is important for designing effective treatments. For example, our work suggests that high IAP protein levels induced by the initial round of treatment could diminish the effectiveness of secondary rounds of treatment. Therefore it could prove beneficial to take a "drug-holiday" until IAP proteins have returned to basal levels before administering additional treatments. This strategy has proved effective for other chemotherapy drugs (Becker et al., 2011; Das Thakur et al., 2013). Additional single-cell approaches measuring anti-apoptotic pathways could help inform dose schedules for optimal drug treatment.

EXPERIMENTAL PROCEDURES

Cell Culture

HCT116 cells were grown in McCoy's with 10% FBS, 100 μg/ml penicillin, 0.25 μg/ml streptomycin, and 85 μg/ml amphotericin. When necessary, McCoy's media was supplemented with 5 μg/ml blasticidin, 50 μg/ml hygromycin, and 0.5 μg/ml puromycin.

Cell Line Construction

Construction of the p53-VKI cell line is described in the Supplemental Experimental Procedures.

To construct the p21 and PUMA reporters, we used multisite gateway cloning (Invitrogen). The p21 promoter sequence (2.4 kb) (el-Deiry et al., 1993) was cloned upstream of ECFP-PEST-NLS sequence in a lentiviral vector with the blasticidin resistance gene. We cloned the two p53 response elements from the PUMA promoter using the PUMA Frag2-Luc plasmid (Yu et al., 2001) upstream of mCherry-PEST-NLS into a lentiviral vector with the hygromycin resistance gene. HCT116 p53-VKI cells were infected with lentivirus containing both reporters as described above and grown in media containing 50 μg/ml hygromycin and 0.5 μg/ml puromycin. Clones were isolated as described above.

Western Blot Analysis

Cells were washed once with 1× PBS and flash frozen in ethanol and dry ice. Cells were lysed in lysis buffer (50 mM Tris pH 7.5, 100 mM NaCl, 1% Triton X-100, 0.5% deoxycholate, 0.1% SDS). We measured protein concentration by a BCA assay (Pierce) and ran equal protein concentrations on 4%–12% Bis-Tris gradient gels (Invitrogen). Protein was transferred to a PVDF membrane and incubated in blocking solution (5% nonfat dried milk, 0.1% Triton X-100, 1× PBS) for 2 hr at room temperature. Membranes were then incubated with primary antibody (in blocking solution) overnight at 4°C. Blots were washed three times for 5 min in washing solution (50 mM Tris-Cl pH 7.5, 150 mM NaCl, 0.05% Tween-20) and then incubated in blocking solution plus secondary antibody coupled to peroxidase (Sigma) for 1 hr. Membranes were washed three times in washing solution, and we detected protein levels with chemiluminescence (ECL Prime GE Healthcare). Molecular weights were identified using a protein standard (Precision Plus, Bio-Rad).

Live-Cell Microscopy

Approximately 10,000 cells were plated in McCoy's media with 10% FBS to poly-D-lysine-coated glass bottom dishes (MatTek). Cells were grown for 72 hr prior to imaging to allow cells to attach to dishes. Before imaging, media was replaced with RPMI without phenol red or riboflavin and supplemented with 5% FBS. Cells were imaged on a Nikon Eclipse TE-2000 inverted microscope in an enclosure to maintain humidity, a temperature of 37°C and 5% CO_2. Images were captured every 30 min using MetaMorph software. Filter sets are listed in the Supplemental Information. Image analysis was performed using ImageJ (NIH) and MATLAB (MathWorks).

Viability Matrix

Using MATLAB, we broke each p53 trajectory into 5-hr time windows. Within each time window, cells were binned according to their maximum integrated p53 levels during that time window. We then determined the proportion of cells in each bin that enacted apoptosis during the experiment and divided this by the total number of cells in each bin to determine the percentage of apoptotic cells in each bin.

Quantitative PCR

Cells were washed one time with PBS and flash frozen in ethanol and dry ice. RNA was extracted using a RNeasy kit (QIAGEN). RNA concentration was determined by measuring absorbance at 260 nm. RNA was converted to cDNA using the high-capacity cDNA kit (Applied Biosystems). Quantitative PCR was performed with 8.4 ng cDNA, 100 nM primer, and SYBR green reagent (Applied Biosystems). Primers are listed in the Supplemental Information.

Viability Assays

Approximately 3,000 cells were plated to each well of a 96-well plate. Drugs were added 24 hr later. Seventy-two hours after drug treatment 100 μl of Cell Titer-Glo reagent (Promega) was added to each well and luminescence was measured by a Victor2 plate reader (PerkinElmer).

SUPPLEMENTAL INFORMATION

Supplemental Information includes Supplemental Experimental Procedures and six figures and can be found with this article online at http://dx.doi.org/10.1016/j.cell.2016.03.025.

AUTHOR CONTRIBUTIONS

A.L.P., J.C.L., W.C.F., and G.L. conceived experiments. A.L.P. performed experiments. A.L. created the HCT116 p53-VKI strain. A.L.P. and J.C.L. analyzed data. A.L.P. and G.L. wrote the paper.

ACKNOWLEDGMENTS

We thank T. Weinert, U. Alon, and S. Gaudet for comments and discussions; G. Gaglia for the p21 promoter construct, S. Chen, J. Stewart-Ornstein, A. Iagovitina, and J. Reyes for advice on figures; J. Porter for support and encouragement; A. Kedves for help with initial cisplatin studies; the Nikon Imaging Center at Harvard Medical School for help with microscopy; and members of the Lahav lab for comments and discussion. This research was supported by Novartis Institutes for Biomedical Research and NIH grant GM083303. A.L.P. was supported by an American Cancer Society New England Division-Ellison Foundation Postdoctoral Fellowship. J.C.L. was supported by the Molecular Biophysics Training Grant (NIH/NIGMS T32008313) and the National Science Foundation Graduate Research Fellowship.

Received: April 7, 2015
Revised: November 25, 2015
Accepted: March 16, 2016
Published: April 7, 2016

REFERENCES

Almendro, V., Marusyk, A., and Polyak, K. (2013). Cellular heterogeneity and molecular evolution in cancer. Annu. Rev. Pathol. *8*, 277–302.

Altena, R., Fehrmann, R.S.N., Boer, H., de Vries, E.G.E., Meijer, C., and Gietema, J.A. (2015). Growth differentiation factor 15 (GDF-15) plasma levels increase during bleomycin- and cisplatin-based treatment of testicular cancer patients and relate to endothelial damage. PLoS ONE *10*, e0115372.

Batchelor, E., Loewer, A., Mock, C., and Lahav, G. (2011). Stimulus-dependent dynamics of p53 in single cells. Mol. Syst. Biol. *7*, 488.

Becker, A., Crombag, L., Heideman, D.A.M., Thunnissen, F.B., van Wijk, A.W., Postmus, P.E., and Smit, E.F. (2011). Retreatment with erlotinib: Regain of TKI sensitivity following a drug holiday for patients with NSCLC who initially responded to EGFR-TKI treatment. Eur. J. Cancer *47*, 2603–2606.

Behar, M., Barken, D., Werner, S.L., and Hoffmann, A. (2013). The dynamics of signaling as a pharmacological target. Cell *155*, 448–461.

Berndtsson, M., Hägg, M., Panaretakis, T., Havelka, A.M., Shoshan, M.C., and Linder, S. (2007). Acute apoptosis by cisplatin requires induction of reactive oxygen species but is not associated with damage to nuclear DNA. Int. J. Cancer *120*, 175–180.

Carvajal, L.A., and Manfredi, J.J. (2013). Another fork in the road–life or death decisions by the tumour suppressor p53. EMBO Rep. *14*, 414–421.

Chen, X., Ko, L.J., Jayaraman, L., and Prives, C. (1996). p53 levels, functional domains, and DNA damage determine the extent of the apoptotic response of tumor cells. Genes Dev. *10*, 2438–2451.

Cohen, A.A., Eden, E., Issaeva, I., Sigal, A., Milo, R., Liron, Y., Kam, Z., Cohen, L., Danon, T., Perzov, N., et al. (2008). Dynamic proteomics of individual cancer cells in response to a drug. Science *322*, 1511–1516.

Das, S., Raj, L., Zhao, B., Kimura, Y., Bernstein, A., Aaronson, S.A., and Lee, S.W. (2007). Hzf Determines cell survival upon genotoxic stress by modulating p53 transactivation. Cell *130*, 624–637.

Das Thakur, M., Salangsang, F., Landman, A.S., Sellers, W.R., Pryer, N.K., Levesque, M.P., Dummer, R., McMahon, M., and Stuart, D.D. (2013). Modelling vemurafenib resistance in melanoma reveals a strategy to forestall drug resistance. Nature *494*, 251–255.

Duale, N., Lindeman, B., Komada, M., Olsen, A.-K., Andreassen, A., Soderlund, E.J., and Brunborg, G. (2007). Molecular portrait of cisplatin induced response in human testis cancer cell lines based on gene expression profiles. Mol. Cancer *6*, 53.

el-Deiry, W.S., Tokino, T., Velculescu, V.E., Levy, D.B., Parsons, R., Trent, J.M., Lin, D., Mercer, W.E., Kinzler, K.W., and Vogelstein, B. (1993). WAF1, a potential mediator of p53 tumor suppression. Cell *75*, 817–825.

Flusberg, D.A., Roux, J., Spencer, S.L., and Sorger, P.K. (2013). Cells surviving fractional killing by TRAIL exhibit transient but sustainable resistance and inflammatory phenotypes. Mol. Biol. Cell *24*, 2186–2200.

Fulda, S., and Vucic, D. (2012). Targeting IAP proteins for therapeutic intervention in cancer. Nat. Rev. Drug Discov. *11*, 109–124.

Hao, N., and O'Shea, E.K. (2011). Signal-dependent dynamics of transcription factor translocation controls gene expression. Nat. Struct. Mol. Biol. *19*, 31–39.

Haupt, Y., Maya, R., Kazaz, A., and Oren, M. (1997). Mdm2 promotes the rapid degradation of p53. Nature *387*, 296–299.

Hoffmann, A., Levchenko, A., Scott, M.L., and Baltimore, D. (2002). The IkappaB-NF-kappaB signaling module: temporal control and selective gene activation. Science *298*, 1241–1245.

Holohan, C., Van Schaeybroeck, S., Longley, D.B., and Johnston, P.G. (2013). Cancer drug resistance: an evolving paradigm. Nat. Rev. Cancer *13*, 714–726.

Hussner, J., Ameling, S., Hammer, E., Herzog, S., Steil, L., Schwebe, M., Niessen, J., Schroeder, H.W., Kroemer, H.K., Ritter, C.A., et al. (2012). Regulation of interferon-inducible proteins by doxorubicin via IFNγ-JAK-STAT signaling in tumor cells. Mol. Pharmacol. *81*, 679–688.

Jiang, M., Wei, Q., Wang, J., Du, Q., Yu, J., Zhang, L., and Dong, Z. (2006). Regulation of PUMA-alpha by p53 in cisplatin-induced renal cell apoptosis. Oncogene *25*, 4056–4066.

Kelland, L. (2007). The resurgence of platinum-based cancer chemotherapy. Nat. Rev. Cancer *7*, 573–584.

Kracikova, M., Akiri, G., George, A., Sachidanandam, R., and Aaronson, S.A. (2013). A threshold mechanism mediates p53 cell fate decision between growth arrest and apoptosis. Cell Death Differ. *20*, 576–588.

Kreso, A., O'Brien, C.A., van Galen, P., Gan, O.I., Notta, F., Brown, A.M., Ng, K., Ma, J., Wienholds, E., Dunant, C., et al. (2013). Variable clonal repopulation dynamics influence chemotherapy response in colorectal cancer. Science *339*, 543–548.

Kuchina, A., Espinar, L., Çağatay, T., Balbin, A.O., Zhang, F., Alvarado, A., Garcia-Ojalvo, J., and Süel, G.M. (2011). Temporal competition between differentiation programs determines cell fate choice. Mol. Syst. Biol. *7*, 557.

Lee, M.J., Ye, A.S., Gardino, A.K., Heijink, A.M., Sorger, P.K., MacBeath, G., and Yaffe, M.B. (2012). Sequential application of anticancer drugs enhances cell death by rewiring apoptotic signaling networks. Cell *149*, 780–794.

Lee, R.E.C., Walker, S.R., Savery, K., Frank, D.A., and Gaudet, S. (2014). Fold change of nuclear NF-κB determines TNF-induced transcription in single cells. Mol. Cell *53*, 867–879.

Liedert, B., Pluim, D., Schellens, J., and Thomale, J. (2006). Adduct-specific monoclonal antibodies for the measurement of cisplatin-induced DNA lesions in individual cell nuclei. Nucleic Acids Res. *34*, e47.

Liston, P., Roy, N., Tamai, K., Lefebvre, C., Baird, S., Cherton-Horvat, G., Farahani, R., McLean, M., Ikeda, J.E., MacKenzie, A., and Korneluk, R.G. (1996). Suppression of apoptosis in mammalian cells by NAIP and a related family of IAP genes. Nature *379*, 349–353.

Loewer, A., Batchelor, E., Gaglia, G., and Lahav, G. (2010). Basal dynamics of p53 reveal transcriptionally attenuated pulses in cycling cells. Cell *142*, 89–100.

Loewer, A., Karanam, K., Mock, C., and Lahav, G. (2013). The p53 response in single cells is linearly correlated to the number of DNA breaks without a distinct threshold. BMC Biol. *11*, 114.

Lopes, R.B., Gangeswaran, R., McNeish, I.A., Wang, Y., and Lemoine, N.R. (2007). Expression of the IAP protein family is dysregulated in pancreatic cancer cells and is important for resistance to chemotherapy. Int. J. Cancer *120*, 2344–2352.

Nakagawa, Y., Abe, S., Kurata, M., Hasegawa, M., Yamamoto, K., Inoue, M., Takemura, T., Suzuki, K., and Kitagawa, M. (2006). IAP family protein expression correlates with poor outcome of multiple myeloma patients in association with chemotherapy-induced overexpression of multidrug resistance genes. Am. J. Hematol. *831*, 824–831.

Nakano, K., and Vousden, K.H. (2001). PUMA, a novel proapoptotic gene, is induced by p53. Mol. Cell *7*, 683–694.

Purvis, J.E., and Lahav, G. (2013). Encoding and decoding cellular information through signaling dynamics. Cell *152*, 945–956.

Purvis, J.E., Karhohs, K.W., Mock, C., Batchelor, E., Loewer, A., and Lahav, G. (2012). p53 dynamics control cell fate. Science *336*, 1440–1444.

Rashi-Elkeles, S., Warnatz, H.-J., Elkon, R., Kupershtein, A., Chobod, Y., Paz, A., Amstislavskiy, V., Sultan, M., Safer, H., Nietfeld, W., et al. (2014). Parallel profiling of the transcriptome, cistrome, and epigenome in the cellular response to ionizing radiation. Sci. Signal. *7*, rs3.

Riley, T., Sontag, E., Chen, P., and Levine, A. (2008). Transcriptional control of human p53-regulated genes. Nat. Rev. Mol. Cell Biol. *9*, 402–412.

Roesch, A., Fukunaga-Kalabis, M., Schmidt, E.C., Zabierowski, S.E., Brafford, P.A., Vultur, A., Basu, D., Gimotty, P., Vogt, T., and Herlyn, M. (2010). A temporarily distinct subpopulation of slow-cycling melanoma cells is required for continuous tumor growth. Cell *141*, 583–594.

Roux, J., Hafner, M., Bandara, S., Sims, J.J., Hudson, H., Chai, D., and Sorger, P.K. (2015). Fractional killing arises from cell-to-cell variability in overcoming a caspase activity threshold. Mol. Syst. Biol. *11*, 803.

Samuels-Lev, Y., O'Connor, D.J., Bergamaschi, D., Trigiante, G., Hsieh, J.K., Zhong, S., Campargue, I., Naumovski, L., Crook, T., and Lu, X. (2001). ASPP proteins specifically stimulate the apoptotic function of p53. Mol. Cell *8*, 781–794.

Shangary, S., and Wang, S. (2009). Small-molecule inhibitors of the MDM2-p53 protein-protein interaction to reactivate p53 function: a novel approach for cancer therapy. Annu. Rev. Pharmacol. Toxicol. *49*, 223–241.

Sharma, S.V., Lee, D.Y., Li, B., Quinlan, M.P., Takahashi, F., Maheswaran, S., McDermott, U., Azizian, N., Zou, L., Fischbach, M.A., et al. (2010). A chromatin-mediated reversible drug-tolerant state in cancer cell subpopulations. Cell *141*, 69–80.

Spencer, S.L., Gaudet, S., Albeck, J.G., Burke, J.M., and Sorger, P.K. (2009). Non-genetic origins of cell-to-cell variability in TRAIL-induced apoptosis. Nature *459*, 428–432.

Tang, Y., Luo, J., Zhang, W., and Gu, W. (2006). Tip60-dependent acetylation of p53 modulates the decision between cell-cycle arrest and apoptosis. Mol. Cell *24*, 827–839.

Tang, Y., Zhao, W., Chen, Y., Zhao, Y., and Gu, W. (2008). Acetylation is indispensable for p53 activation. Cell *133*, 612–626.

Tenev, T., Bianchi, K., Darding, M., Broemer, M., Langlais, C., Wallberg, F., Zachariou, A., Lopez, J., MacFarlane, M., Cain, K., and Meier, P. (2011). The Ripoptosome, a signaling platform that assembles in response to genotoxic stress and loss of IAPs. Mol. Cell *43*, 432–448.

Tirrò, E., Consoli, M.L., Massimino, M., Manzella, L., Frasca, F., Sciacca, L., Vicari, L., Stassi, G., Messina, L., Messina, A., and Vigneri, P. (2006). Altered expression of c-IAP1, survivin, and Smac contributes to chemotherapy resistance in thyroid cancer cells. Cancer Res. *66*, 4263–4272.

Toettcher, J.E., Weiner, O.D., and Lim, W.A. (2013). Using optogenetics to interrogate the dynamic control of signal transmission by the Ras/Erk module. Cell *155*, 1422–1434.

Varfolomeev, E., Blankenship, J.W., Wayson, S.M., Fedorova, A.V., Kayagaki, N., Garg, P., Zobel, K., Dynek, J.N., Elliott, L.O., Wallweber, H.J., et al. (2007). IAP antagonists induce autoubiquitination of c-IAPs, NF-kappaB activation, and TNFalpha-dependent apoptosis. Cell *131*, 669–681.

Vassilev, L.T. (2007). MDM2 inhibitors for cancer therapy. Trends Mol. Med. *13*, 23–31.

Vassilev, L.T., Vu, B.T., Graves, B., Carvajal, D., Podlaski, F., Filipovic, Z., Kong, N., Kammlott, U., Lukacs, C., Klein, C., et al. (2004). In vivo activation of the p53 pathway by small-molecule antagonists of MDM2. Science *303*, 844–848.

Vazquez, A., Bond, E.E., Levine, A.J., and Bond, G.L. (2008). The genetics of the p53 pathway, apoptosis and cancer therapy. Nat. Rev. Drug Discov. *7*, 979–987.

Vince, J.E., Wong, W.W.-L., Khan, N., Feltham, R., Chau, D., Ahmed, A.U., Benetatos, C.A., Chunduru, S.K., Condon, S.M., McKinlay, M., et al. (2007). IAP antagonists target cIAP1 to induce TNFalpha-dependent apoptosis. Cell *131*, 682–693.

Vucic, D., Stennicke, H.R., Pisabarro, M.T., Salvesen, G.S., and Dixit, V.M. (2000). ML-IAP, a novel inhibitor of apoptosis that is preferentially expressed in human melanomas. Curr. Biol. *10*, 1359–1366.

Young, J.W., Locke, J.C.W., and Elowitz, M.B. (2013). Rate of environmental change determines stress response specificity. Proc. Natl. Acad. Sci. USA *110*, 4140–4145.

Yu, J., Zhang, L., Hwang, P.M., Kinzler, K.W., and Vogelstein, B. (2001). PUMA induces the rapid apoptosis of colorectal cancer cells. Mol. Cell *7*, 673–682.

Zhu, Y., Regunath, K., Jacq, X., and Prives, C. (2013). Cisplatin causes cell death via TAB1 regulation of p53/MDM2/MDMX circuitry. Genes Dev. *27*, 1739–1751.